

Electroplating of conformal electrodes for vacuum nanogap tunnel junction

Larissa Jangidze, Avto Tavkhelidze*, Jujin Blagidze, and Zaza Taliashvili

Tbilisi State University, Chavchavadze Ave. 13, 0179 Tbilisi, Georgia

**E-mail: avtotav@geo.net.ge*

In this study, we electroplated Cu electrode on Si substrate to achieve a large-area vacuum nanogap for thermotunnel devices. We used cathode coating, cathode rotation, asymmetric current regime, and electrolyte temperature regulation and stabilization to obtain the regular geometry of the Cu electrode and reduce its internal tension. On the first stage, we achieved Cu of 450–750 μm thickness, with the thickness difference between center and perimeter as low as 7 μm . Subsequently, we regulated the internal tension of the Cu to obtain the predefined surface curvature (concave or convex). For 12-mm diameter Ag/Cu, we obtained a minimum curvature of 40 nm/mm from the Ag side. Reduction of the diameter to 3 mm allowed the growth of Ag/Cu with curvature as low as of 2.5 nm/mm. It also allowed fabrication of two conformal electrodes having a nanogap of <5 nm width, over the area of 7 mm². Such conformal electrodes could be used for devices based on electron tunneling.

Keywords: electrochemical growth of Cu, conformal surfaces, electron tunneling, thermotunneling

Introduction

In recent years, the work on fabrication of micro-coolers based on quantum-mechanical tunneling of the electron has been in progress [1–6]. The first theoretical study of cooling by tunneling was made to avoid overheating in the single-electron transistors [1]. The typical metal/insulator/metal (MIM) tunnel junction has high heat conductivity owing to low insulator thickness (3–10 nm). This results in a parasitic heat backflow, which decreases the cooling coefficient. The metal/vacuum/metal (MVM) tunnel junction is free from this drawback, but at the same time is very complex from the standpoint of practical feasibility. However, a conformal electrodes method that allows one to obtain a large-area vacuum nanogap has been proposed [2]. The method is based on electrochemical growth of conformal electrodes. The characteristics of refrigerators with vacuum nanogap were theoretically studied in a number of earlier researches [3–7]. It was shown that the cooling power for the MVM junction is of the order of 100 W/cm^2 [3, 5]. However, the cooling coefficient of such junctions does not exceed 10%. In an earlier study [6], a metal/vacuum/insulator/metal (MVIM) tunnel junction having additional thin insulator-on-collector layer was examined. The cooling coefficient of such a junction turned out to be much higher, of the order of 40–50% and, in addition, the insulator layer protected the electrodes against short circuit and simplified their design. The method of practical realization of conformal electrodes by Cu electroplating was also investigated [8].

Methods and experimental results

We used *n*-type Si(100) double-sided polished substrates having the diameter of 50, 40, and 20 mm, and a thickness of 1–2 mm for the base electrode. Thin Ti and Ag (Ti – 0.1 μm and Ag – 1.2 μm) films were deposited on the Si wafer in vacuum, in situ, with low adhesion between them. However, the adhesion between Ti and Ag films was regulated precisely [9]. Subsequently, the sample was exposed to the atmosphere and the thick copper layer was electroplated on a silver surface.

Thick Cu layers were deposited in the sulfate electrolyte ($\text{CuSO}_4 \cdot 5\text{H}_2\text{O} + \text{H}_2\text{SO}_4 + \text{C}_2\text{H}_5\text{OH} + \text{H}_2\text{O}$) in the thermo-stabilized bath, at the current density $J=(15\text{--}50) \text{ mA/cm}^2$, with mechanical stirring of the electrolyte. The electrolyte used is not complex in its composition, is stable and can be easily corrected, allowing the use of relatively high current densities, and the current output becomes close to the theoretical value – 100%. The ethyl alcohol prevents, to some extent, the formation of one-valence copper ions, thereby resulting in dense, finely crystalline precipitates. The current lead was connected to the Si wafer from the back side that was insulated from the electrolyte.

The electrolysis was carried out in the thermo-stabilized bath in the temperature range of 23.5–35°C. Temperature stabilization in the process of electrolysis is necessary to exclude the influence of different thermal extraction coefficients of the Si wafer and the deposited Cu layer. To stabilize the temperature of the electrolyte, two baths were used. The internal bath with electrolyte was placed in the external bath with water. In the external bath, the water temperature was maintained by means of a heater and was 2°C lower than that in the internal bath. The temperature of the electrolyte inside the internal bath was varied in the range of 23.5–35°C, and stabilized with an accuracy of 0.3°C. Our first task was to obtain a uniform surface of the deposited Cu to form a metal electrode of the required diameter and shape. The following ways were used to control the Cu distribution over the cathode surface:

- Coating of the cathode surface with the ring masks of electrically insulating material of different geometries
- Placing additional cathodes near the main cathode
- Cathode rotation
- Use of anodes of different sizes
- Use of the asymmetric alternating current

Copper electrode having a diameter of $D=28$ mm was deposited on 50-mm and 40-mm diameter Si wafers. In addition, the electrodes with diameters of 12 and 3 mm were developed on 20-mm diameter wafers. The Cu thickness was 450–750 μm for the diameters of 28 and 12 mm, and up to 4000- μm thickness for the 3 mm diameter.

As a result, a Si/Ti/Ag/Cu sandwich was formed (Fig. 1a). Subsequently, the sandwich was opened and the bulk Si/Ti and Ag/Cu conformal electrodes were obtained (Fig. 1b). The sandwich was heated or cooled to separate the electrodes [2] using difference in the thermal expansion of Si and Cu.

The surface conformity (i.e., the absolute curvature value) of the electrodes formed after splitting was evaluated by the optical method on the Ag/Cu electrode from the Ag side, using a Michelson interferometer [10]. The He–Ne laser with the wavelength of $\lambda=632.8$ nm served as a light source. One of the interferometer mirrors was replaced by the mirror-surface of the Ag/Cu electrode. The interference pattern was formed in the air gap between one of the mirrors and a virtual image of the second mirror (sample in our case). When the gap was plane-parallel, fringes of equal inclination (circular rings) were obtained (Fig. 2). After fixing

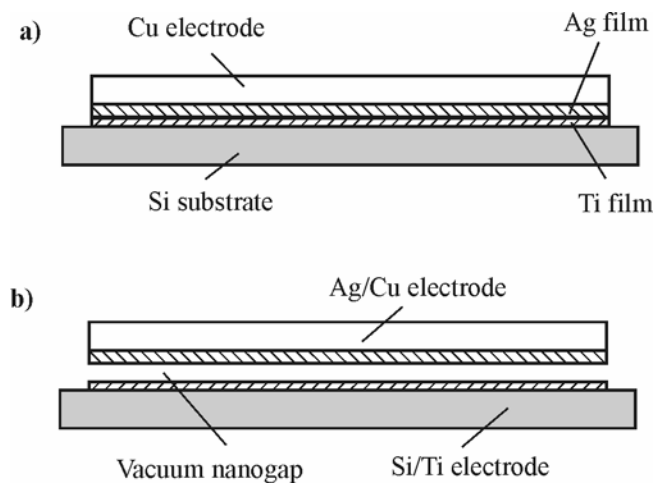


Fig. 1 a). Multilayer sandwich Si/Ti/Ag/Cu; b) Sandwich after opening, Si/Ti and Ag/Cu electrodes are separated.

the sample on a particular plate of the interferometer, the sample was adjusted to obtain an interference pattern with equal inclination fringes. By counting the number of rings, n , the absolute curvature of the sample can be calculated using the formula, $N=n \times \lambda/2$. The sign of the curvature was determined by slightly pressing the longer leg of the mirror. Unbending of the rings in the interference pattern indicates surface convexity and consequently, bending of the rings shows concavity. To determine a normalized curvature of the metal electrode, the formula $\alpha=n(\lambda/2)/D$ was used. The initial normalized curvature for base electrode (Si wafers) of $D=50$, 40, and 20 mm was 57, 47, and 16 nm/mm, respectively. The temperature was monitored during the interferometer measurements of the curvature and was kept equal to the Cu electrode growth temperature.

In the initial experiments, the copper surface was highly non-uniform, with bulging edges (Fig. 3a). The copper thickness at the electrode edges was nearly twice as much as in the

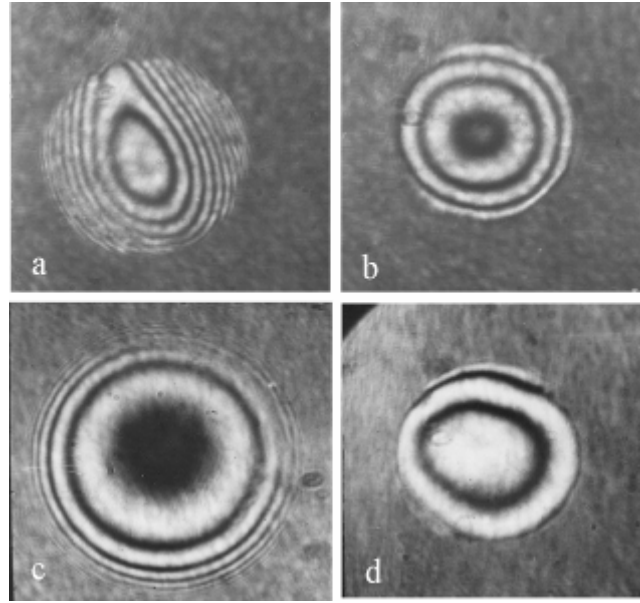


Fig. 2 a). Ag/Cu electrode (from the Ag side) with $D=12$ mm deposited without the cathode rotation; b) Ag/Cu electrode (from the Ag side) with $D=12$ mm deposited with the cathode rotation; c) Si/Ti electrode surface with $D=20$ mm; d) Ag/Cu electrode surface with $D=12$ mm (from the Ag side).

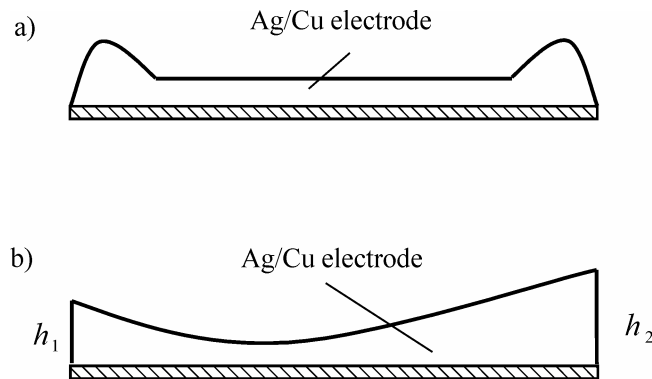


Fig. 3 a). Ag/Cu electrode deposited without a protective mask, b) Ag/Cu electrode deposited with a protective mask of 3-mm height.

middle of the electrode. In contrast to the theoretical estimation that only yields the average thickness on the whole covered surface, it was experimentally demonstrated [11] that even on the flat electrodes placed at equal distances from the anodes, the current density and the coating thickness were distributed non-uniformly: the current density was much higher than that estimated in the corners and edges, and lower in the middle part. In the case of two parallel electrodes of equal area placed in an electrolyte, the current passed not only along the main field lines (normal to the electrode surface), but also along the additional field lines (not normal to the surface). If the electrodes were placed in parallel to each other and the electrolyte cross-section had an area that was more than that of the electrodes, however, the power lines were more or less concentrated at the electrode edges and bent around them depending on the electrode and the bath geometry.

To remove the edge defects during the deposition of copper of $D=28$ mm with the thickness, $h = 45\text{--}750$ μm , different protective masks of 3-mm thickness were used. The Ag/Cu electrode copper layer had a concave Cu surface with different edge thicknesses (Fig. 3b). The copper-layer thickness

in the lower part of the electrode h_2 was always higher than that in the upper part of the electrode h_1 . The average difference was $\Delta h_{av}=105 \mu\text{m}$. The Ag surface of 28-mm diameter Ag/Cu electrode had a curvature of cylindrical shape with an average value of 237 nm/mm for the relative curvature.

To eliminate the Ag/Cu electrode curvature, the Si wafer diameter was reduced to 20 mm, with the wafer thickness being unchanged, i.e., 1 mm, and the deposited electrode diameter was decreased to 12 mm. To reduce the Δh_{av} for the 12-mm diameter Ag/Cu electrode, the thickness of the ring protection mask was increased up to 10 mm. The Cu surface retained a similar concave shape with different edge heights, but the value of Δh_{av} decreased to 41 μm . On the other hand, the Ag surface of the electrode had the same cylindrical relief and the normalized curvature value was 178 nm/mm (Fig. 2a). It is known that during metal electroplating, the precipitates exhibit mechanical tension and when deposition takes place only on one side of the cathode; these tension forces lead to the cathode curvature [12]. Therefore, to decrease the cathode curvature, we decided to increase the Si wafer thickness to up to 2 mm. As a result, the electrode curvature decreased and the following values were obtained: for Ag/Cu electrode with $D=12$ mm, the relative curvature was 117 nm/mm. The comparison of the curvature of the metal electrodes deposited on the Si wafers of 1 and 2 mm thickness showed that in the case of 2-mm wafer, the Ag/Cu electrode curvature decreased nearly 1.5 times. To reduce the non-uniformity of the edges of the electrode, additional cathodes were placed near the main cathode. In the case of Cu electrode of $D=12$ mm, the additional ring electrode was placed on the outer diameter of the ring protective mask. The additional electrode overtook the part of the current, and substantially reduced the Cu non-uniformity at the edges. The current density of additional cathode was $J=5 \text{ mA/cm}^2$. The Cu surface became essentially more uniform with $\Delta h_{av}=9 \mu\text{m}$, $N_{av}=3.3$ rings, and the relative electrode curvature was 87 nm/mm (measured from Ag side).

To further reduce the electrode surface nonuniformity, we rotated the cathode. Rotation also provided electrolyte steering. It resulted in copper surface with uniform edges, centrally symmetrical metal electrode curvature (Fig. 2b), and the required curvature sign. In addition, the cone protective masks of 5 and 10 mm height, with hole diameters of 9/12, 10/12, 11/12, 12/12 mm, respectively, were used. Depending on the protective mask, the hole diameter, and angular velocity of cathode rotation, either concave (Fig. 4a) or convex (Fig. 4b) copper surface of the Cu electrode was obtained. For 9/12 mm and 10/12 mm masks, the copper surface was always convex, irrespective of the angular velocity of the cathode rotation. For the 11/12 mm and 12/12 mm mask at $V_\phi=2.5$ rpm, the copper surface was essentially concave, whereas, at $V_\phi=10$ rpm, it was convex (here, V_ϕ depicts angular velocity of the cathode rotation). The average Δh_{av} , Δl_{av} , and α_{av} values are given in Table 1. Here, Δl is the difference in the thickness of the electrode between center and the edges (Fig. 4a).

As Table 1 shows, the minimum relative curvature is obtained for 10/12 mask. Besides the standard-size copper anodes (having an area twice as much as the cathodes), flat $D=10$ mm and

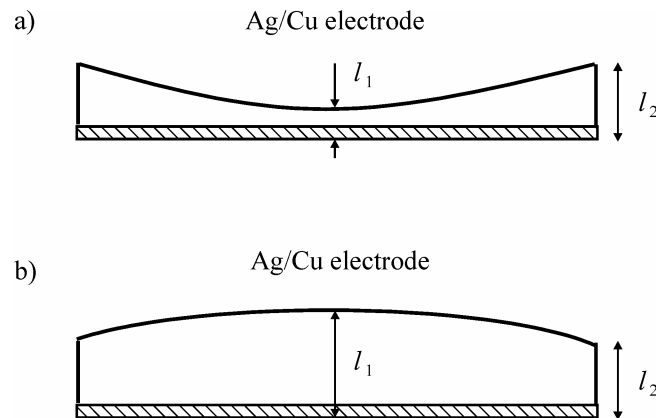


Fig. 4. Ag/Cu electrodes deposited with cone mask and rotating cathode: a) walleye Cu surface; b) hill Cu surface.

tapered $D=8$ mm anodes were also used. In the case of $V_\phi=0$ and with the standard protective mask of 10-mm height, we obtained $\Delta h_{av}=13$ μm . The introduction of taped masks and cathode rotation did not lead to substantial changes in this particular case. To improve the surface curvature, we used AC having different amplitudes of direct and reverse currents. In an earlier study [13], 80–90%

Table 1. Values of Δh_{av} , Δl_{av} , and α_{av} in the case of $D=12$ mm electrodes with cone masks.

Min/max hole diameters	2.5 rpm		10 rpm		α_{av} [nm/mm]
	Δh_{av} [μm]	Δl_{av} [μm]	Δh_{av} [μm]	Δl_{av} [μm]	
9/12	10.5	115	12	149	126
10/12	3.7	45.5	5	89	84
11/12	7.4	9.4	10.7	75	210
12/12	4.1	46	5.9	39.5	195

of AC current period was used to grow Cu, and the rest was used to flatten the surface in the reverse current regime. We applied asymmetric AC with an amplitude of (0.35–1.15) mA and an asymmetry of 40–90% to the additional cathode at the frequency of 20, 30, and 50 Hz. For $V_\phi=0$, we obtained a concave Cu surface with $\Delta l_{av}=36$ μm and an Ag surface curvature of 132 nm/mm.

For the deposition of thick Cu layers (450–750 μm), the asymmetric AC with an amplitude of (30–35) mA was used together with the protective mask of 5-mm thickness and a hole diameter of 12 mm. In this case, the most uniform Cu surface with $\Delta l_{av}=8.4$ μm and the relative curvature from Ag side of 158 nm/mm was obtained at $V_\phi=10$ rpm.

It is well known that the increase in the electrolyte temperature accelerates the process of deposition of the thick copper layer and introduces substantial changes —salt solubility and electric conductivity of the electrolyte increase, the anode passivity decreases, the ion-diffusion conditions improve, and the internal stress reduces. Besides, its precipitates become more plastic, leading to better conservation of curvature sign and shape of electrodes after sandwich splitting. However, the cathode polarization decreases and the precipitates of the macro-crystalline structure start to grow at higher temperatures, which could be compensated by the increase in the current density and electrolyte stirring [14, 15]. To investigate the temperature dependence of the relative curvature of Cu electrode of 12-mm diameter, the electrode was grown using cone protective mask of 10-mm height and hole diameter of 10/12 mm. The cathode rotation speed was $V_\phi=10$ rpm and the current density was $J=(25\text{--}30)$ mA/cm². At high temperatures of 40–45°C, the sandwiches split during the electrolysis process, and therefore, the experiments were carried out within the limited temperature range of 23.5–35°C. The curvature dependence on electrolyte temperature for the 12 mm Ag/Cu electrode is given in Fig. 5. As figure indicates the value of the electrode

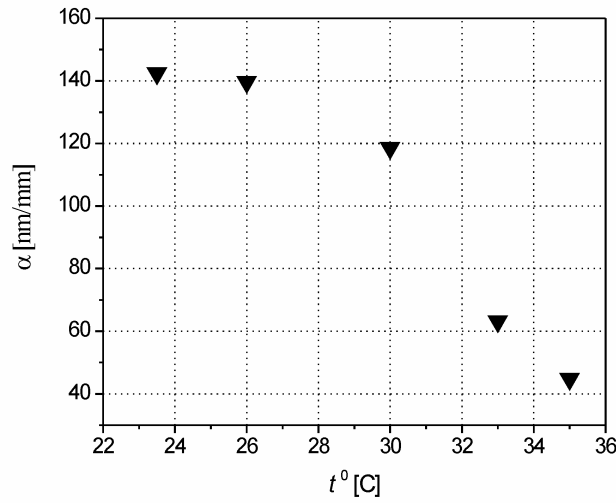


Fig. 5. Dependence of normalized curvature on electrolyte temperature for Ag/Cu electrode with $D=12$ mm.

curvature decreases nearly three times with the increasing temperature. Fig. 2 shows interferograms of c) Si/Ti and d) Ag/Cu electrodes, after opening of sandwich grown at 35°C.

In the next stage, we decreased the Cu electrode diameter to 3 mm. The copper was deposited with the thickness from 700 to 2300 μm with the cathode rotation of 2.5 rpm and 10 rpm. The current density was 15–20 mA/cm^2 , and both the DC and AC regimes were used. Table 2 indicates that during the formation of the Ag/Cu metal electrode of $D=3$ mm, the best result, $\alpha_{\text{av}}=40$ nm/mm, was obtained by applying the asymmetric AC with a rotation speed of 10 rpm.

Table 2. Δh_{av} , Δl_{av} , and α_{av} values for the Ag/Cu electrode with $D=3$ mm in the case of DC and AC.

	2.5 rpm		10 rpm		α_{av} [nm/mm]
	Δh_{av} [μm]	Δl_{av} [μm]	Δh_{av} [μm]	Δl_{av} [μm]	
DC	-	-	3	6.7	74
AC	18.5	13.9	11	7.3	40

We also grew copper of $D=3$ mm of up to 4000 μm thickness. In this case, the asymmetric AC density was increased to $J=(30-0)$ mA/cm^2 and the Cu was deposited with $V_\phi=2.5$ rpm, using the protective mask of 5-mm thickness. Two extreme electrolyte temperatures of 23.5°C and 35°C were investigated. The results are given in Table 3. The dependence on

Table 3. Curvature values of the Ag/Cu electrode with $D=3$ mm for the electrolyte temperatures, 23.5°C and 35°C

α [nm/mm] for samples grown at $t=23.5^\circ\text{C}$	<2.5	<2.5	17.9	4.2	<2.5	<2.5
α [nm/mm] for samples grown at $t=35^\circ\text{C}$	105.4	7.3	4.2	8.4	34.8	3.2

temperature was quite different for the Ag/Cu electrode with $D=3$ mm, compared with the Ag/Cu electrode with $D=12$ mm, and with increasing electrolyte temperature, the normalized curvature also increased. This can be ascribed to structural differences. We used high temperature and high current density to reduce the growth time for 4000- μm thick Cu. Because of high growth speed, the copper precipitates were of poor quality – fragile and porous, sometimes with dendrites, which affect the Ag/Cu electrode curvature. It is known from the literature [16] that with increasing thickness of the precipitate, the size of the grains gradually increases and then stabilizes at particular thicknesses. This in turn reduces the internal stress values to a certain constant value. It is also known that with further increase in thickness, the internal stresses in the copper precipitate gradually, which decreases depending on the electrolysis regime [17]. We chose high current density $J=(30\text{--}40)$ mA/cm² for thick electrode growth at 23.5°C. This way, we reduced the curvature down to 2.5 nm/mm, and in some cases, the samples without any curvature, i.e., samples with maximum electrode conformity were obtained.

The basic problem after sandwich opening was the surface conformity of the two electrodes – Si/Ti and Ag/Cu. Initially, the vast majority of Si substrates were convex (owing to mechanical polishing). In the process of Cu growth, the Si wafer was deformed in one or another direction with respect to the initial curvature. After the sandwich splitting, the Si wafer restored to its initial curvature, and the Ag/Cu metal electrode could be both concave (Fig. 6a) or convex (Fig. 6b). Hence, our task was to obtain a concave Ag/Cu electrode surface. We investigate the

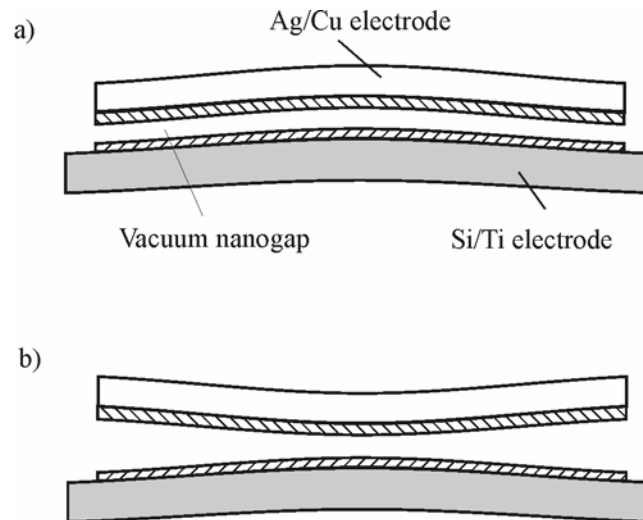


Fig. 6. Sandwich after opening: a) Si/Ti electrode is convex and Ag/Cu electrode is concave; b) Si/Ti electrode is convex and Ag/Cu electrode is convex.

dependence of the curvature sign (i.e., the fraction of concave and convex surfaces in percentage terms) of the Ag/Cu electrode on the thickness of the Si wafer and the electrolyte temperature. When the copper was deposited on Si wafers of 1-mm thickness, the number of concave surfaces was 22%, and for copper deposition on Si wafers of 2-mm thickness, the number of concave surfaces was 59%. Obviously, the increase in the wafer thickness enhances the number of concave surfaces to nearly 2.7 times. The results of the curvature-sign dependence on temperature are given in Table 4, for 2-mm thick Si wafer and electrode diameters of 12 mm and 3 mm. Table 4 shows that the best results for the 12-mm and 3-mm Ag/Cu electrodes were obtained for the electrolyte temperatures $t=33^\circ\text{C}$ and 35°C , and $t=23.5^\circ\text{C}$, respectively.

We evaluated the contact area between the Si/Ti and Ag/Cu electrode surfaces. The contact area of the electrode surfaces replicating each other (i.e., Si/Ti surface is convex and

Table 4. Fraction of concave surface of Ag/Cu electrodes having diameters of 12 and 3 mm at different temperatures.

	Ag/Cu with $D=12$ mm					Ag/Cu with $D=3$ mm	
t (°C)	23.5	26	30	33	35	23.5	35
Concave surfaces (%)	54	24	26	80	82	100	85.7

Ag/Cu surface is concave) can be estimated from simple geometry [10,18]. For this purpose, we considered the cross-section of the sandwich in a plane perpendicular to its surface and crossing its center (Fig. 7). The region where the distance between the electrodes is $\delta \leq 50$ Å can be

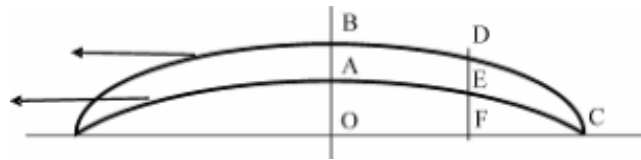


Fig. 7. Sandwich cross-section: AEC – Si/Ti electrode surface, BDC – Ag/Cu electrode surface.

defined as a surface contact. Subsequently, the contact area is the area of the ring with external radius equal to the sample radius OC, and the internal radius OF. By replaced AC and BC arcs by straight lines with sufficient degree of accuracy, we found that the contact area could be expressed by the formula: $S = \pi r^2 (\delta/H) (2 - \delta/H)$. Here, AB is the difference between the surface maximum curvature, $AB = H$ and $DE = \delta$. The presented evaluations of the contact area between the Si/Ti and Ag/Cu electrode surfaces for some samples of $D=3$ mm diameter electrodes are given in Table 5. The value of $\delta=5$ nm was used for calculation and H was determined from $H = n \times \lambda$, where n was the measured number of rings.

Table 5 shows that the best results for the contact area between the Si/Ti and Ag/Cu electrode surfaces, which were obtained in the process for the electrolyte temperature $t = 23.5^\circ\text{C}$. For three samples, the whole area of the electrodes is contact area, signifying that the vacuum nanogap has a width of < 5 nm on the whole area of the electrodes.

Table 5. The number of interference rings and the corresponding contact area for the Ag/Cu electrodes with $D=3$ mm.

]

$t=23.5^{\circ}\text{C}$		$t=35^{\circ}\text{C}$	
n number of rings (ring count)	S contact area mm^2	n number of rings (ring count)	S contact area mm^2
<0.025	6–7	1	0.2
<0.025	6–7	0.07	2.8
0.17	1.22	0.04	4.42
0.04	4.42	0.08	2.48
<0.025	6–7	0.33	0.65
0.025	6.05	0.03	5.4

Conclusions

In the process of conventional electroplating of a thick Cu, we used protective masks with a thickness of 10 mm to reduce the difference in the Cu thickness at the electrode edges by a factor of 2.5. Cathode rotation allowed to obtain a central-symmetric curvature of the electrode, and also allowed the change of the sign of the curvature to the required direction. The increase in the Si wafer thickness from 1 mm to 2 mm allowed us to reduce the normalized curvature of Cu electrode by a factor of 1.5 and increase the output of concave Ag/Cu electrodes with $D=12$ mm by 37%. At the same time, with increasing electrolyte temperature from $t = 23.5\text{--}35^{\circ}\text{C}$, the relative curvature decreases to 44.8 nm/mm, and the output of the concave surfaces increases by 28%.

By reducing the Ag/Cu electrode diameter to $\varnothing 3$ and using the asymmetric AC, the relative curvature of the metal electrode was reduced down to 2.5 nm/mm. At $t=23.5^{\circ}\text{C}$, all the surfaces of the obtained samples were concave and the samples with no measurable electrode surface curvature were obtained (<2.5 nm/mm). Calculation of the surface area (on the basis of the experimental values of curvatures) revealed that the nanogap between the electrodes was <5 nm on the whole surface of the 3-mm diameter electrodes.

Thus, electroplated conformal surfaces can be used as electrodes in the vacuum nanogap thermotunnel refrigerators and power generators.

Acknowledgments

This work has been funded and supported by Borealis Technical Ltd., the assignee of corresponding US Patents: 7,253,549; 7,208,021; 7,169,006; 7,140,102; 6,971,165; 6,876,123; 6,969,855, 6,774,003; 6,720,704; 6 281 514; 6 495 843; 6 680 214; 6 531 703; 6 117 344.

References

1. A.N. Korotkov, M.R. Samuelsen, S.A. Vasenko, J. Appl. Phys., 76 (6), p. 3623-3631 (1994).
2. A. Tavkhelidze, G. Skhiladze, A. Bibilashvili, L. Tsakadze, L. Jangidze, Z. Taliashvili, I. Cox, and Z. Berishvili, Proc. XXI International Conf. on Thermoelectric, August 26–29 IEEE, New York, pp. 435–438 (2002).
3. Y. Hishinuma, T. H. Geballe, B. Y. Moyzhes, and T. W. Kenny Appl. Phys. Lett. 78, 2572 (2001).
4. T. Zeng, Appl. Phys. Lett. 88, 153104 (2006).
5. Zhang Xin and Zhang Dian-Lin, Chinese Phys. 16, 2656-2660 (2007).
6. Avto Tavkhelidze, Vasiko Svanidze, and Leri Tsakadze, J. Vac. Sci. Technol. A, v.26(1), p.5 (2008) .
7. Hishinuma I., Geballe T.H., Moyzhes B.I., Kenny T.W. Appl. Phys. Lett. v, 94(7), p. 4690 (2003).
8. L.B.Jangidze, A.N.Tavkhelidze, M.O.Tetradze and T.D.Devidze , Methods for Improving Surface Flatness in Thick Cu Film Electrodeposition, Russian Microelectronics, v. 36(2), pp. 116-119 (2007).
9. Z. I. Taliashvili, L. R. Vardosanidze, L. B. Jangidze, and A. N. Tavkhelidze Control of the Adhesion Strength of Thin Metal Films in Multilayer Structures, Russian Microelectronics, v. 36(5), p. 313 (2007).
10. Frish S.E. *Opticheskie metody izmerenia* (Optical Measurement Techniques), part 2, *Luchevaia optika i granitsy ee primeneniya* , (Ray optics and its Limits), Leningrad: Lening.Gos.Univ.,p. 226 (1980).
11. Lainer V.I, *Zashchitnye pokrytia metallov*, (Protective Coating on Metals), Moscow, Metallurgiya, p. 559 . (1974).
12. Vagramyan A.T. et al., *Fizico-mekhanicheskie svoistva elektroliticheskikh osadkov*, (Physical and Mechanical Properties of Electrodeposits), Moscow: Izdatel'stvo AN USSR, p. 206 (1960).
13. Dasoyan M.A., Pal'mskaya I.Ya. and Sakharova E.V., *Tekhnologiya elektrokhimicheskikh pokrytii* (Electrochemical Coating Processes), Leningrad: Mashinostroenie, p. 390 (1989).
14. Vairner Ya.V. and Dasoyan M.A. *Tekhnologiya elektrokhimicheskikh pokrytii* (Electrochemical Coating Processes), Mashinostroenie, p. 464 (1972).
15. Gindlin V.K., *Galvanotekhnika v poligrafii*, (Galvanotechnics in polygraphy), Izdatel'stvo Kniga, p. 324 (1965).
16. Povetkin V.V. and Kovenskii I.M. *Struktura elektroliticheskikh pokrytii*, (Electrochemical Coating Structures), Moscow: Metallurgiya, p. 136 (1989).
17. Popereka M.Ya., *Vnutrennie napryazheniya elektroliticheski osazhdennykh metallov*, (Internal Stress of Electrodeposited Metals), Novosibirsk: Zapadnosibirskoe Knizhnoe Izdatel'stvo, p. 335 (1966).
18. Landsberg G.S. *Optika*, (Optics), Moscow: Nauka, p. 926 (1967).